Journal of Bioenergetics and Biomembranes, Vol. 34, No. 6, December 2002 (© 2002)

Cross-Linking of the Endogenous Inhibitor Protein (IF_1) With Rotor (γ, ε) and Stator (α) Subunits of the Mitochondrial ATP Synthase

Fernando Minauro-Sanmiguel,[1] Concepción Bravo,[1] and José J. García[1,2]

Received October 15, 2002; accepted October 16, 2002

The location of the endogenous inhibitor protein (IF_1) in the rotor/stator architecture of the bovine mitochondrial ATP synthase was studied by reversible cross-linking with dithiobis(succinimidylpropionate) in soluble F_1I and intact F_1F_0I complexes of submitochondrial particles. Reducing two-dimensional electrophoresis, Western blotting, and fluorescent cysteine labeling showed formation of α–IF_1, IF_1–IF_1, γ–IF_1, and ε–IF_1 cross-linkages in soluble F_1I and in native F_1F_0I complexes. Cross-linking blocked the release of IF_1 from its inhibitory site and therefore the activation of F_1I and F_1F_0I complexes in a dithiothreitol-sensitive process. These results show that the endogenous IF_1 is at a distance $\leq$12 Å to γ and ε subunits of the central rotor of the native mitochondrial ATP synthase. This finding strongly suggests that, without excluding the classical assumption that IF_1 inhibits conformational changes of the catalytic β subunits, the inhibitory mechanism of IF_1 may involve the interference with rotation of the central stalk.

KEY WORDS: ATP synthase; inhibitor protein; IF; rotor; stator; cross-linking.

INTRODUCTION

The F_1F_0-ATP synthase is a rotational motor enzyme that provides most of the ATP required in all species. Experimentally, the enzyme can be separated in soluble (F_1) and membranal (F_0) portions. F_0 works as a proton channel, and the soluble F_1 is the catalytic moiety that preserves the capacity to hydrolyze ATP. In the intact ATP synthase, F_1 and F_0 are structurally and functionally coupled through two stalks. The central stalk forms part of the rotor of the enzyme, and the peripheral stalk is part of the stator that anchors the catalytic sites of F_1 to the membrane (for recent reviews, see Boyer, 2000; Capaldi and Aggeler, 2002; García *et al.*, in press; Noji and Yoshida, 2001).

Because the whole ATP synthase is a reversible motor, it can work as ATPase or ATP synthase. The enzyme is controlled in physiological conditions by the so-called inhibitor protein (IF_1) to prevent ATP hydrolysis. Therefore, the functional form of the mitochondrial ATP synthase *in vivo* is that containing its endogenous IF_1, i.e., the F_1F_0I complex (Vázquez-Contreras *et al.*, 1995). Since its first isolation in 1963 by Pullman and Monroy (1963), several laboratories have studied the properties of IF_1 as the intrinsic inhibitor of the ATPase activity of the enzyme. The binding stoichiometry of IF_1 is 1 per ATP synthase (Hashimoto *et al.*, 1981; Klein *et al.*, 1980). Most of the available structural data show the cross-linking of IF_1 with α (Mimura *et al.*, 1993) and β (Beltrán *et al.*, 1988; Jackson and Harris, 1988; Klein *et al.*, 1980, 1981) subunits of F_1; however, cross-linking, activity, and assembly

Key to abbreviations: CAPS, 3-(ciclohexylamino)-1-propanesulfonic acid; CPM, 7-diethylamino-3-(4′-maleimidylphenyl)-4-methylcoumarin; DCCD, dicyclohexylcarbodiimide; DSP, dithiobis (succinimidylpropionate); DTT, dithiothreitol; EDTA, ethylenediamine-tetraacetic acid; F_1, the soluble F_1-ATPase; F_0, the membranal proton channel of the ATP synthase; F_1I, the complex of soluble F_1-ATPase containing the inhibitor protein; F_1F_0I, the native ATP synthase containing the inhibitor protein; IF_1, the inhibitor protein of the mitochondrial ATP synthase; FRET, fluorescence resonance energy transfer; mAb, monoclonal antibody; NMR, nuclear magnetic resonance; SDS-PAGE, denaturing sodium dodecyl sulphate polyacrylamide gel electrophoresis; SMP, submitochondrial particles.

[1]Departamento de Bioquímica, Instituto Nacional de Cardiología, "Ignacio Chávez," México, D.F. 14080, México.

[2]To whom correspondence should be addressed at Departamento de Bioquímica, Instituto Nacional de Cardiología, Juan Badiano #1, Col. Sección XVI, México D.F. 14080, México; e-mail: jjgarcia_trejo@yahoo.com.

0145-479X/02/1200-0433/0 © 2002 Plenum Publishing Corporation

studies (García *et al.*, 2000; López-Mediavilla *et al.*, 1993; Papa *et al.*, 2000) suggest interactions of IF_1 with F_0 subunits. The soluble F_1 containing IF_1 can be isolated as the so-called F_1I complex whose latent ATPase activity is recovered after activation in conditions of high-ionic strength and pH (Klein *et al.*, 1982; Pullman and Monroy, 1963), i.e., conditions similar to those required for activation of the whole F_1F_0I complex. Circular dichroism (Lebowitz and Pedersen, 1993, 1996; Van Heeke *et al.*, 1993; Van Raaij *et al.*, 1990), NMR (Gordon-Smith *et al.*, 2001), and crystallographic (Cabezón *et al.*, 2001) analyses of recombinant rat liver and bovine soluble IF_1s show a high content of α-helix that decreases at acidic pH where it exerts a stronger inhibition. Recently, it has been shown that these changes are associated to a shift in the aggregation state of soluble IF_1 from a noninhibitory tetramer to an inhibitory IF_1 dimer (Cabezón *et al.*, 2000a). Furthermore, it has been also shown that the soluble F_1I complex containing the reconstituted (Cabezón *et al.*, 2000b) or endogenous (Domínguez-Ramírez *et al.*, 2001) IF_1 exists preferentially in a dimerized form that is induced by formation of IF_1 dimers (Cabezón *et al.*, 2000b).

Several studies have shown intrinsic differences between the reconstituted and the endogenous IF_1 (Feinstein and Moundrianakis, 1984; Fornells *et al.*, 1998; Galante *et al.*, 1981; Krull and Schuster, 1981; Schwerzmann *et al.*, 1982; Valdés and Dreyfus, 1987). Therefore, we studied the location of the endogenous IF_1 in the soluble F_1I and in the intact ATP synthase. Chemical modification of F_1I and F_1F_0I with dithiobis(succinimidylpropionate) (DSP) formed novel cross-linkages of IF_1 with γ and ε subunits, i.e., components of the central rotor that controls the conformational changes of the catalytic α/β interfaces (Aggeler *et al.*, 1997; Boyer, 2000; Capaldi and Aggeler, 2002; Duncan *et al.*, 1995; García *et al.*, in press; Gibbons *et al.*, 2000; Kato-Yamada *et al.*, 1998; Noji *et al.*, 1997; Noji and Yoshida, 2001; Sabbert *et al.*, 1996; Tsunoda *et al.*, 2001). Therefore, these findings strongly suggest that IF_1 may not only inhibit the conformational changes of the catalytic β subunits as it has been inferred from previous cross-linking results (Beltrán *et al.*, 1988; Jackson and Harris, 1988; Klein *et al.*, 1980; Mimura *et al.*, 1993); IF_1 could also interfere with rotation of the central stalk to inhibit ATP hydrolysis.

MATERIALS AND METHODS

Bovine heart mitochondria and "Mg-ATP" submitochondrial particles (SMP) were prepared as described before (García *et al.*, 1995). Soluble F_1-ATPase and the F_1I complex containing the endogenous IF_1 were purified from SMP by affinity chromatography with Sepharose-EAH (Pharmacia) as described elsewhere (Tuena de Gómez-Puyou and Gómez-Puyou, 1977). Soluble F_1I was activated by incubation in media containing Tris-SO_4, 50 mM; EDTA, 2 mM; KCl, 100 mM; and ATP, 10 mM (pH 8.0) at 40°C for 90 min. ATPase activity was measured spectrophotometrically as described before (García *et al.*, 1995).

Cross-linking of the F_1F_0I complex in SMP and of soluble F_1I with DSP. Cross-linking experiments were carried out with DSP (Pierce), a DTT-reversible and homo-bifunctional reactant that forms highly specific cross-linkages between lysines that are at about 12 Å proximity. To form cross-linkages between neighboring subunits of the ATP synthase, SMP or soluble F_1I were incubated at concentrations of 1 or 4 mg or protein/mL, respectively, with the indicated concentrations of DSP. For soluble F_1I, the cross-linking buffer was 20 mM KH_2PO_4, pH 7.0, whereas for the SMP it also included 250 mM sucrose. The reaction was carried out for 30 min at room temperature and arrested with 20 mM L-lysine.

Reducing 2D SDS-PAGE after nonreducing 1D SDS-PAGE. First, F_1I subunits and their cross-linked products were separated in a nonreducing 1D (10–22%) SDS-PAGE (Laemmli, 1970). Afterwards, the lanes containing the samples of interest were excised from the gels as fragments of the indicated range of molecular weights and incubated 1 h with 20 mM DTT (Gibco) at room temperature in 0.1% SDS (Biorad). Subsequently, the cut lanes were washed three times with 0.1% SDS to remove residual DTT and re-electrophoresed in a 2D (10–22%) SDS-PAGE. Lane fragments were horizontally layered on the top of 2D gels; a stacking gel was polymerized between the excised lane and the separating gradient gel. Two spacers were included at the sides of the layered excised lane for appropriate standards.

Immunoprecipitation of F_1F_0I solubilized from SMP. The F_1F_0I complex was immunoprecipitated from SMP with a new monoclonal antibody named 12F4AD8 described elsewhere (Aggeler *et al.*, 2002). This antibody immunoprecipitates the whole, native, functional, and oligomycin-sensitive F_1F_0I complex (Aggeler *et al.*, 2002). SMP at 1.5 mg of protein/mL were first solubilized in lauryl maltoside buffer (20 mM Mes-Tris (pH 6.8), 150 mM sucrose, 1 mM ADP, and 2.25 mg/mL lauryl maltoside). The mixtures were centrifuged for 45 min at 45,000 rpm at 4°C. The soluble portion was incubated with control Protein-G beads coupled to nonspecific antibodies (NSA) of preimmune mice antiserum for 1 h at room temperature. Afterwards, the beads were pelleted and the supernatant was incubated with the monoclonal antibody 12F4AD8 coupled to Protein-G beads for

2 h at room temperature. At this point, the coupled beads were washed five times with 20 mM Mes-Tris (pH 6.8), 150 mM sucrose, 1 mM ADP, 0.05% lauryl maltoside. Finally, the immunoprecipitated F_1F_0I complex was eluted with glycine 100 mM, pH 2.5, and the pH was readjusted to 7.5 with phosphate buffer.

Immunodetection of cross-linked subunits. SDS-PAGE was carried out under nonreducing (without DTT) and reducing (+20 mM DTT) conditions. Afterwards, proteins were transferred 2 h to PVDF membranes at 100 mA in a buffer containing 100 mM CAPS, 10% methanol (pH 11.0). For immunodetection of IF_1, mAb raised against recombinant rat liver IF_1 (García *et al.*, 2000) was used. The recombinant rat liver IF_1 was overexpressed in *Escherichia coli* and purified as described elsewhere (García *et al.*, 2000; Lebowitz and Pedersen, 1993). Immunodetection of subunit α was carried out with another mAb as described before (García *et al.*, 2000). A polyclonal antibody raised against bovine γ subunit was also used and it was a generous gift of Professors M. Tuena de Gómez-Puyou and A. Gómez-Puyou. Reactive bands were immunodetected with secondary goat anti-mouse or goat anti-rabbit IgGs conjugated to HRP and the chemiluminescent ECL-Plus kit of Amersham-Pharmacia.

Fluorescent labeling of accessible cysteines of α, γ, and ε subunits with CPM. Labeling with coumarin maleimide (CPM, Mol. Probes) was carried out for 2 min at room temperature by using a concentration of 5 mg/mL of F_1I complex and 100 μM of CPM in 25 mM potassium phosphate at pH 7.0. The labeling reaction was arrested by column centrifugation (Penefsky, 1979). Fluorescent CPM-labeled subunits were detected after 1D or 2D SDS-PAGE by exciting CPM in an UV transiluminator. A standard or digital photo camera stored the images. After CPM labeling, DSP cross-linking was carried out as described earlier.

Other methods and materials. The amount of protein in SMP, F_1F_0I, and F_1I preparations was measured with the method of Lowry *et al.* (1951). Densitometric analyses of Coomassie-stained bands in SDS-PAGE gels were carried out with the digital camera and imaging software "ALPHADIGIDOC" of Alpha Innotech Corporation according to the manufacture's instructions. In each gel the molecular weights of cross-linking products were calculated from interpolation by using the appropriate standards. The intensities of subunits were measured by peak integration after densitometry analyses relative to controls nontreated with DSP. Coupling enzymes and substrates for ATPase activity were obtained from Sigma. Reactants for SDS-PAGE were obtained from Biorad laboratories.

RESULTS

The functional integrity of our preparation of soluble F_1I was determined by activation assays. The basal ATPase activity of 2–3 μmol/min/mg increased to 50–70 μmol/min/mg after F_1I was activated as described under Materials and Methods. By comparison, the basal F_1-ATPase activity of the soluble F_1 lacking IF_1 was also 50–70 μmol/min/mg. We used 0.1–2.0 mg/mL of DSP and looked for a DTT-reversible inhibition of IF_1 release (ATPase activation) to find an optimal DSP concentration to cross-link IF_1 with neighboring subunits. In correlation with parallel Western blotting analyses using the mAb against IF_1 (not shown), we found maximal DTT reversibility in ATPase activation and Western analyses at 1 mg/mL DSP. Therefore, this concentration of DSP was used for all experiments shown with soluble F_1I.

DSP cross-linking products in the soluble F_1I complex as detected by Coomassie blue staining of SDS-PAGE. After cross-linking of soluble F_1I with 1 mg/mL DSP, non-cross-linked and cross-linked F_1I were subjected to reducing and nonreducing SDS-PAGE. After Coomassie staining, statistical densitometric analyses showed that the intensities of IF_1, γ, and ε subunits diminished upon cross-linking in a DTT-sensitive process (Fig. 1(A) and 1(B)). Figure 1(A) shows a representative gel where these intensity changes can be observed by eye. Several DTT-sensitive high-molecular products appeared above α and β subunits (not shown), but their nature was not explored. However, two DTT-sensitive faint bands of 36.0 and 43.0 kDa appeared reproducibly in the DSP cross-linked F_1I between α and β subunits (Fig. 1(A), second lane from left to right labeled with *). The DTT-reversible decrease of IF_1 (10 kDa), ε (6 kDa), and γ (30 kDa) intensities suggested that the 36- and 43-kDa products corresponded to γ–ε and γ–IF_1 cross-linkages, respectively.

Identification of the γ–IF_1 cross-linked product in the soluble F_1I complex and resolution of two more γ cross-linked products by 2D SDS-PAGE. To obtain a better resolution of the cross-linked subunits of the F_1I complex, reducing 2D SDS-PAGE was carried out after overloading and overrunning a nonreducing 1D SDS-PAGE with 300 μg of protein per lane. Each lane was excised as a fragment expanding the 25–70-kDa range before reducing it with DTT and loading it into a minigel. As control, cross-linked F_1-ATPase lacking IF_1 was also analyzed under identical conditions. Cross-linked subunits can be identified as vertically aligned spots under the diagonal formed by non-cross-linked subunits and residual cross-linking products. The identity of cross-linked subunits was determined by the vertical position of the spots relative to a non-cross-linked F_1I standard. In soluble F_1 two γ spots

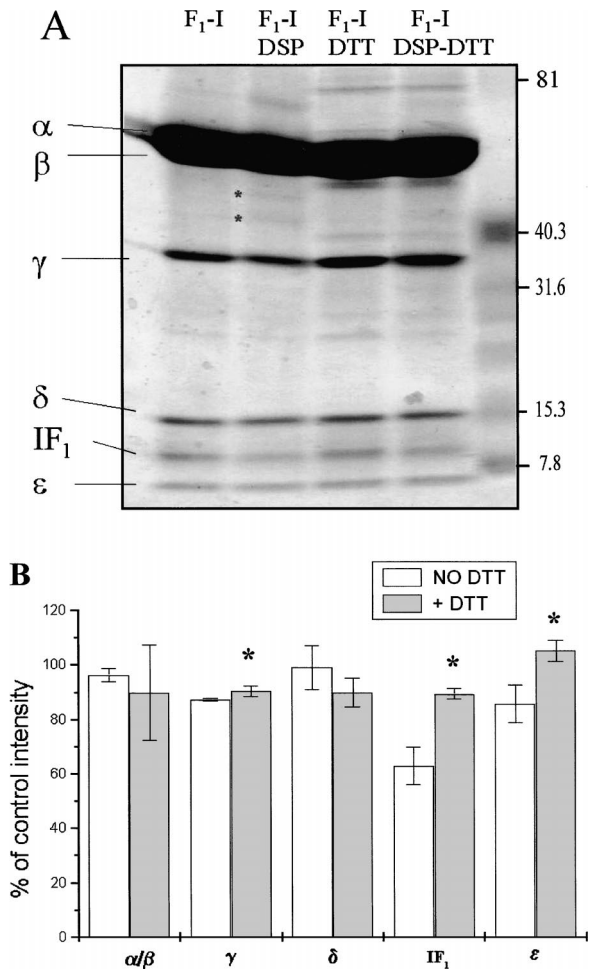

Fig. 1. DSP cross-linking of the F_1I complex forms DTT-sensitive cross-linkages between subunits IF_1, ε, and γ as shown by Coomassie-stained SDS-PAGE. (A) F_1I was cross-linked with 1 mg/mL of DSP as described under Materials and Methods. Afterwards, 60 μg of control and cross-linked samples were loaded in each lane of a 10–22% SDS-PAGE with and without 20 mM DTT. DSP induced the formation of two products of about 36 and 43 kDa that are not observed after DTT reduction (*). Satistical densitometric analyses of three different experiments and F_1I preparations (B) showed that subunits IF_1I, γ and ε are diminished in the cross-linked sample (without DTT), and their intensity is recovered after DTT reduction. One hundred percent corresponds to the intensity of the respective band in the non-cross-linked F_1I standard. Statistical significance of the differences between samples with and without DTT was calculated with the *U* values of the nonparametric Meann Withney method. These values were $\alpha/\beta = 0.513$, $\gamma = 0.05$, $\delta = 0.275$, $IF_1 = 0.05$, $\varepsilon = 0.05$; therefore, statistically significant differences were observed for subunits γ, IF_1, and ε (labeled with *).

were vertically aligned to ε and δ, respectively; the latter was too weak to appear in Fig. 2(A), but it was detected by densitometry analysis (not shown). In contrast, in the cross-linked F_1I complex an additional γ spot appeared between those observed in F_1 (Fig. 2(B)). This spot was vertically aligned to IF_1. A second IF_1 spot at the left side of the gel aligned vertically to α subunit. Western blot of 2D gels loaded with lower amounts of cross-linked F_1I, indicated that IF_1 aligned vertically under two cross-linked IF_1 products of 66 and 43 kDa (Fig. 2(C)). Taken together, the results showed that the product of 36 kDa is a γ–ε cross-link, that of 43 kDa is γ–IF_1, and that of 66 kDa is α–IF_1.

To confirm the identity of these cross-linked subunits, the accessible cysteines of γ, ε, and α subunits were fluorescently labeled with CPM. Subunits β, δ, and IF_1 lack cysteines, and therefore, they are not CPM-labeled. F_1I was first labeled with CPM and afterwards cross-linked with 1 mg/mL of DSP. Two-dimensional SDS-PAGE loaded with 300 μg of protein showed a fluorescent smearing along the diagonal due to α and γ subunits and residual cross-linking products. Under this diagonal, the three fluorescent γ spots were observed together with the fluorescent ε spot aligned in the position of the γ–ε product (Fig. 2(D)). As expected from their lack of cysteines, no fluorescence was detected in the IF_1 and δ spots under the other two γ spots.

To resolve smaller F_1I cross-linking products, the nonreducing first dimension lane containing 400 μg of cross-linked F_1I was excised as a fragment from about 100 kDa to the bottom front. This excised lane was subjected to reducing 2D SDS-PAGE in a large gel. The resulting 2D gel showed several aligned spots clearly defined under the diagonal of F_1I subunits (Fig. 3). Three γ spots were vertically aligned to ε, IF_1, and β subunits, from right to left in order of ascending molecular weights. The γ spot aligned to δ (Fig. 2) was not resolved, presumably because the first dimension gel was not overrun. Four IF_1 spots were vertically aligned to ε, none, γ, and α subunits. These results confirmed the identity of the 43- and 66-kDa cross-linked products as γ–IF_1 and α–IF_1, respectively. They also show formation of the previously observed γ–ε cross-linkage (Joshi and Burrows, 1990, and Fig. 2). Of significant relevance was the presence of ε–IF_1 and IF_1–IF_1 cross-linkages clearly observed in the lower right part under the diagonal (Fig. 3). Similar analyses carried out with a control non-cross-linked F_1I showed, as expected, no spots under the diagonal of F_1I subunits (not shown). Taken together, these results confirm unequivocally the formation of cross-linkages of IF_1 with the rotor subunits γ and ε, together with other products, i.e., α–IF_1, γ–β, and IF_1–IF_1.

Immuno-identification of γ–IF_1 and α–IF_1 cross-linked products formed by DSP in soluble F_1I complex. After cross-linking of soluble F_1I with 1 mg/mL of DSP, Western blotting revealed with the mAb against IF_1 showed formation of four IF_1 cross-linked products of

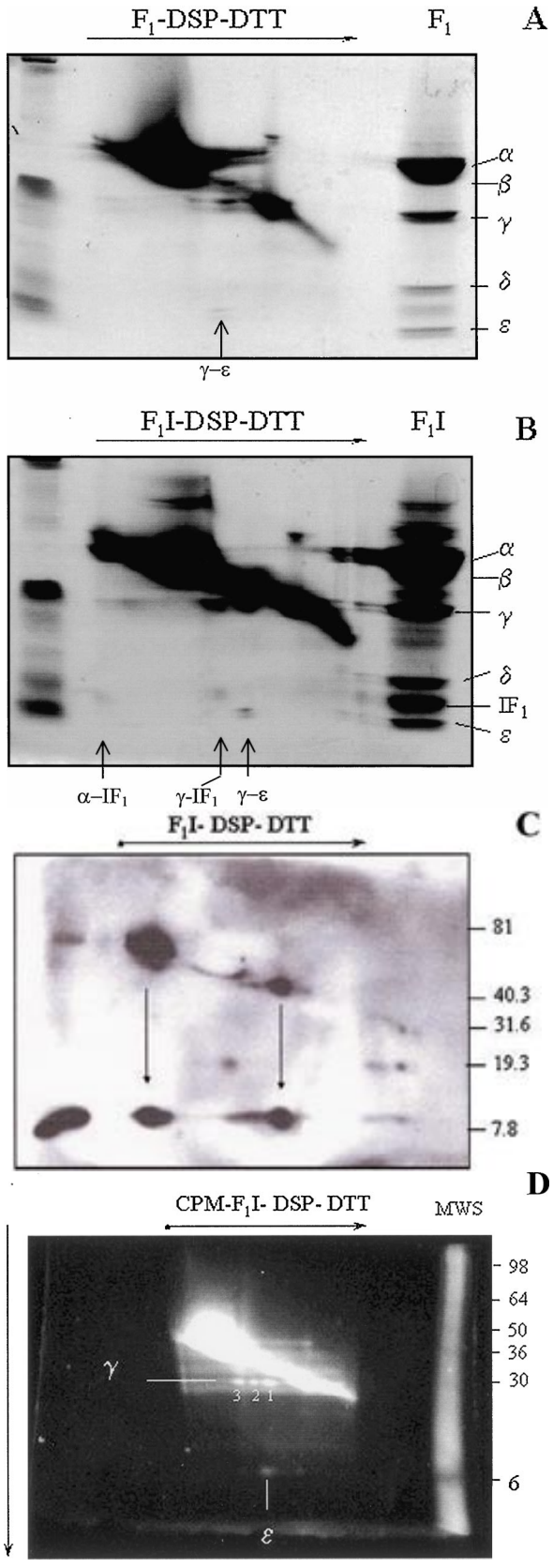

approximately 16, 20, 43, and 66 kDa that were reduced with DTT (Fig. 4, left). The band of about 66 kDa corresponds to the α–IF_1 cross-linked product (Fig. 3), whereas that of 43-kDa results from the γ–IF_1 cross-linkage. The 20-kDa IF_1 product is the cross-linked IF_1 dimer (Fig. 3), whereas the product of 16 kDa corresponds to the ε–IF_1 cross-linkage (Fig. 3).

To confirm the identity of the subunits cross-linked with IF_1 in the 43- and 66-kDa products, Western blotting of control and cross-linked F_1I complexes was carried out using polyclonal and mAbs directed against γ and α subunits, respectively. The two cross-linking products of 43 and 66 kDa revealed with γ (Fig. 4, center) and α (Fig. 4, right) antibodies, respectively, aligned horizontally with the corresponding IF_1 products (Fig. 4, left). These products were completely reduced with DTT, except for the α–IF_1 product which was reduced partially (Fig. 4, left and right). Other cross-linking products of γ and α subunits were observed, including a γ product of 36 kDa corresponding to the γ–ε cross-linkage (Figs. 2 and 3). Larger products containing the α subunit were also observed (Fig. 4, right), but these were not further analyzed.

Cross-linking of the native F_1F_0I-ATP synthase with DSP in SMP. We also studied if the endogenous IF_1 cross-links with rotor subunits of the whole intact F_1F_0I-ATP synthase. For this purpose, SMP were incubated with 5–500 μg/mL DSP and cross-linking products containing IF_1 were detected by Western blotting with the mAb against IF_1 after 1D nonreducing SDS-PAGE (Fig. 5(A)). At low DSP concentrations (5–30 μg/mL, Fig. 5(A)), the α-IF_1 (66 kDa) and γ–IF_1 (43 kDa) were the predominant cross-linking products formed in the native F_1F_0I complex of SMP. At higher DSP concentrations (50–500 mg/mL),

Fig. 2. Identification of subunits cross-linked by DSP in F_1I by 2D SDS-PAGE. Reducing 2D (10–22%) SDS-PAGE after a nonreducing ID was carried out with 300 μg of F_1(A) and F_1I(B) previously cross-linked with 1 mg/mL DSP as described under Materials and Methods. In both cases, the lane of interest was excised from the first dimension as a fragment from about 70–25 kDa that was loaded into the second dimension after DTT reduction. In F_1, two γ spots appeared under the diagonal. The larger spot was vertically alinged (cross-linked) to ε (arrow). In the F_1I complex, a third γ product appeared, which was vertically aligned to IF_1. The identification of IF_1 located under the third γ spot was corroborated by immunoblotting with an IF_1 monoclonal antibody (C) where the products with IF_1 can be detected (arrows). The standard left lane was loaded with 1.0 μg of purified rat liver IF_1, (D) After CPM modification and DSP cross-linking (see Materials and Methods), 300 μg of F_1I was processed for reducing 2D SDS-PAGE showing the three γ spots. Only the ε subunit was labeled and aligned under the first γ spot (from right to left), since δ and IF_1 lack cysteines. The fluorescence along the diagonal is due to overloading and labeling of α, γ, and residual non-reduced cross-linking products.

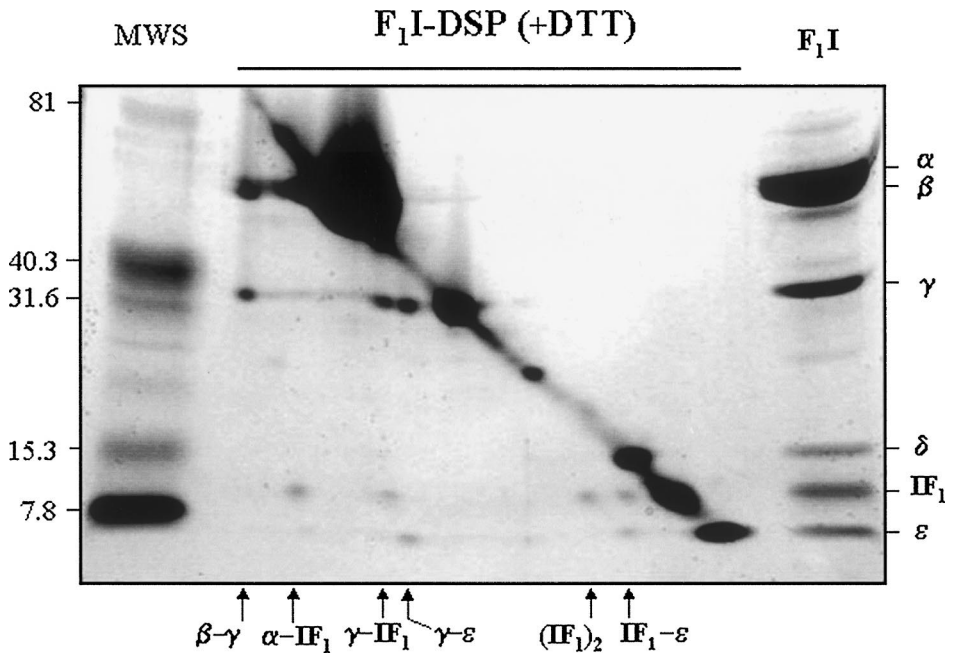

Fig. 3. Reducing 2D SDS-PAGE of DSP cross-linked F_1I complex after a first nonreducing SDS-PAGE. Soluble F_1I complex was cross-linked with 1 mg/mL DSP. Subsequently, 400 μg of cross-linked F_1I was loaded in a single lane of a nonreducing 10–22% gel. Afterwards, the lane was excised as a fragment from about 100 kDa to the bottom and incubated with DTT before loading it horizontally in a large 2D (10–22%) SDS-PAGE gel. The right lane was loaded with control soluble F_1I as standard, and the left lane with molecular weight standards. The gel was stained with Coomassie blue.

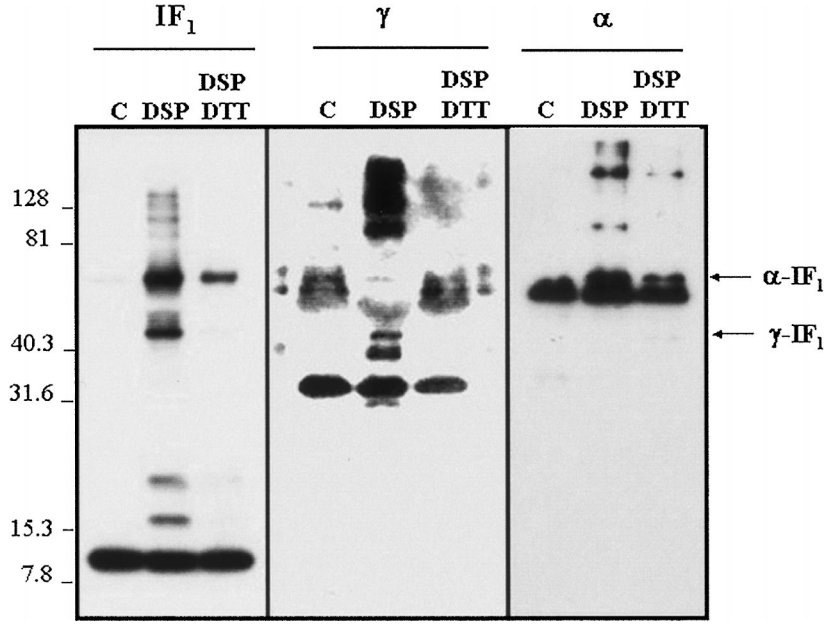

Fig. 4. Immuno-identification of γ–IF_1 and α–IF_1 cross-linking products in soluble F_1I. For immunodetection of IF_1, γ, and α subunits, 1, 20, and 0.5 μg of control, cross-linked, and cross-linked with DTT F_1I were loaded as indicated in a linear 12% ID SDS-PAGE. Afterwards, Western blotting was carried out as described under Materials and Methods using subunit specific monoclonal (IF_1, α) and polyclonal (γ) antibodies as indicated.

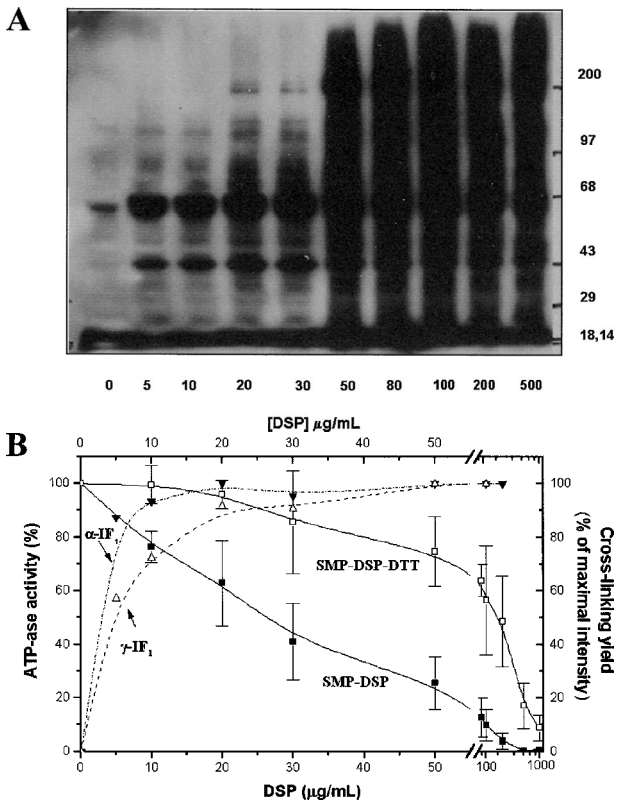

Fig. 5. Formation of IF_1 cross-linking products by DSP correlates with DTT-reversible inhibition of IF_1 release from native F_1F_0I complex in SMP. (A) SMP were cross-linked with the DSP concentrations shown as described under Materials and Methods. After arresting the cross-linking with L-lysine, 30-μg samples were loaded in each lane of a 10–22% SDS-PAGE. The cross-liked products were identified by immunoblotting with the mAb against IF_1. (B) After cross-linking of F_1F_0I in SMP at 1 mg/mL, samples were diluted 10-fold in activation medium with (□) and without (■) DTT and incubated at 40°C for 90 min. Afterwards, the ATPase activity was measured spectrophotometrically. The 100% of activated ATPase activities with and without DTT were in the range of 10–12 μmol/min/mg, and the basal activities before activation were 0.8–1.2 μmol/min/mg. The plot also shows the yield of α–IF_1 and γ–IF_1 cross-linkages relative to the maximal intensity integrated by densitometry analysis at their respective positions of 66 and 43 kDa from the Western blot (A). These intensities were saturated at about 50 μg/mL (B).

a smear of IF_1 bands indicated nonspecific cross-linking. In this gel, the smaller IF_1 products (IF_1–IF_1 and IF_1–ε) were stacked with the main IF_1 band, but they were resolved after immunoprecipitation of the F_1F_0I complex (Fig. 6(B)). It is relevant to point out that at low DSP concentrations (5–30 μg/mL) the yield of α–IF_1 and γ–IF_1 cross-linkages increased progressively whereas the DTT reversibility of the inhibition of ATPase activation by DSP was higher than 80% (Fig. 5(B)). Because the DTT-reversible inhibition of the ATPase activity by DSP has been previously associated with intra- or intermolecular cross-linkages (Kandpal and Boyer, 1987), this indicates that formation of γ–IF_1 and α–IF_1 cross-linkages occurs in a functional fraction of enzymes where IF_1 release, i.e., ATPase activation, is restored by reduction with DTT. The overall inhibition of ATPase activity can be also associated with other cross-linkages not involving IF_1 (see, for example, Joshi and Burrows, 1990, and Fig. 6(C)). This is more evident at higher DSP concentrations where the reversibility by DTT declines (Fig. 5(B)) and formation of nonspecific cross-linkages increases (Fig. 5(A)). Saturation of the Western-blot signal (Fig. 5(B)) might underestimate the calculated yield of α–IF_1 and γ–IF_1 at concentrations of DSP > 50 μM, which actually increases in the immunoprecipitated enzyme (Fig. 6(B)). This would shift the curves of cross-linking yield to the right, therefore improving the correlation with activation assays.

Detection of DSP cross-linked products containing IF_1 in the immunoprecipitated F_1F_0I complex. According to the previous data, cross-linking was carried out in SMP with 25 and 100 μg/mL of DSP. Afterwards, the fully functional F_1F_0I-ATP synthase (Aggeler *et al.*, 2002) was solubilized and immunoprecipitated as explained under Materials and Methods. Coomassie staining of the SDS-PAGE showed a clean preparation of control and cross-linked F_1F_0I complexes (Fig. 6(A)). Reducing and nonreducing SDS-PAGE of the DSP cross-linked samples showed a DTT-sensitive Coomassie-stained band of about 36 kDa (Fig. 6(A)) that corresponded to the γ–ε cross-linkage found in F_1I (Figs. 2 and 3). High-molecular weight and DTT-sensitive cross-linked bands were also present (see Fig. 6(A), above α and β subunits). As with soluble F_1I, the nature of these products was not ascertained.

Western blotting with the monoclonal against IF_1 (Fig. 6(B)) confirmed the presence of the γ–IF_1 (43 kDa) cross-linked product that was observed in soluble F_1I, and in whole SMP (Fig. 5). It was important to show that the 43-kDa γ–IF_1 band disappeared almost completely after DTT reduction (Fig. 6(B)). In contrast, although the ε–IF_1 (16 kDa), IF_1–IF_1 (20 kDa), and α–IF_1 (66 kDa) products were also observed in immunoprecipitated F_1F_0I (Fig. 6(B)), their reversibility by DTT was lower than in soluble F_1I and they were also present in the non-cross-linked enzyme. This may result from insoluble IF_1 aggregates that are also obseved in the purified recombinant IF_1 (Fig. 6(D)). The extent of cross-linking increased with 100 μg/mL of DSP. In this case, smearing was not observed, as was the case for SMP (Fig. 5). Presumably the nonspecific IF_1 products formed in SMP were eliminated after solubilization and immunoprecipition. Further 2D SDS-PAGE carried out before (Fig. 6(A)) and after Western blotting against IF_1 (Fig. 6(B)) confirmed the presence of the α–IF_1 (66 kDa), γ–IF_1 (43 kDa), and γ–ε

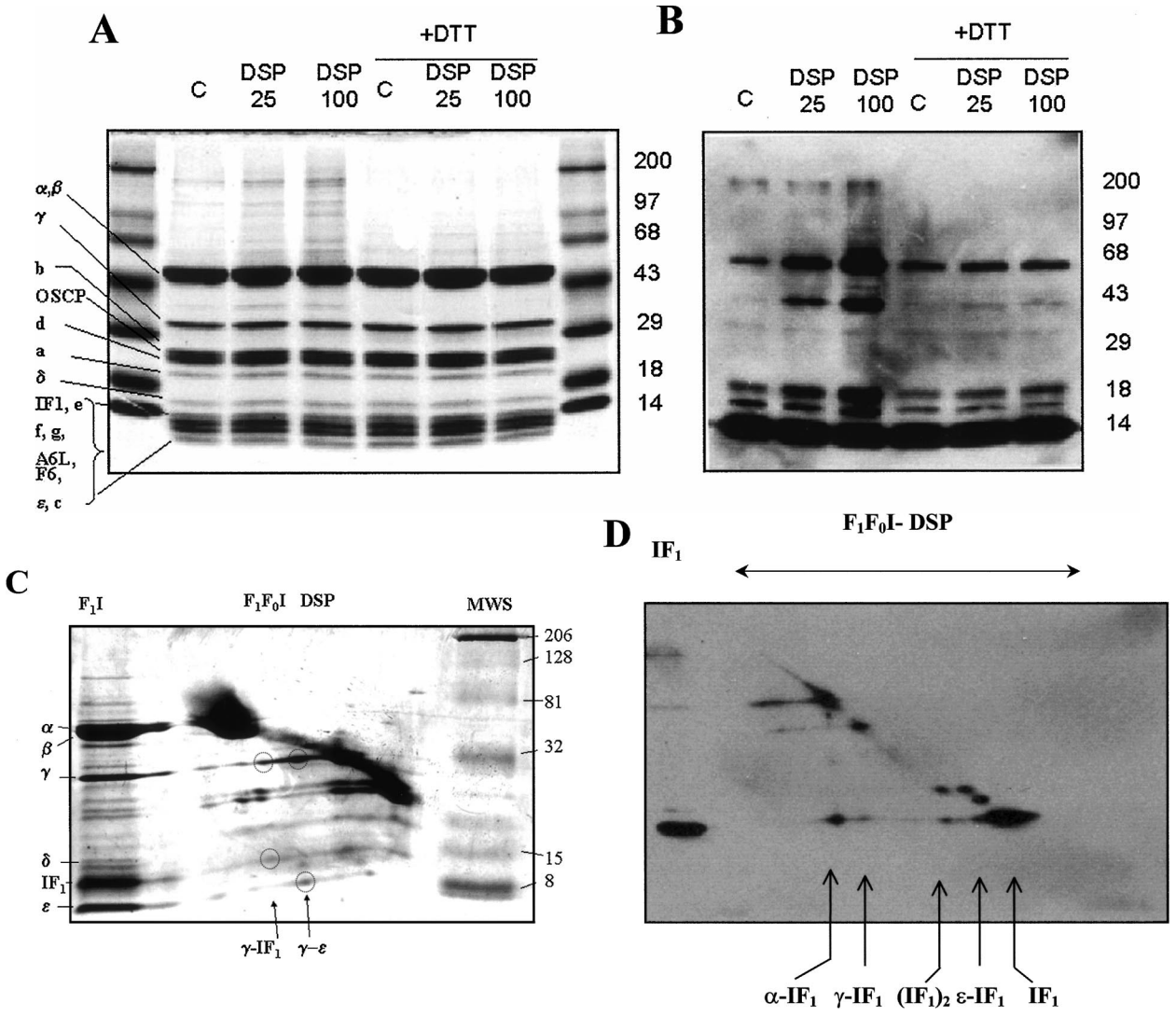

Fig. 6. Detection of γ–IF_1, ε–IF_1, and α–IF_1 cross-linking products in the native F_1F_0I complex by 1D and 2D SDS-PAGE, and Western blotting. SMP were incubated with 25 μg and 100 μg/mL of DSP as described before, and F_1F_0I was solubilized and immunoprecipitated as described under Materials and Methods. (A) Coomassie staining of 30 μg/lane of control ("C") and F_1F_0I cross-linked with 25 and 100 μg/mL DSP (named "25" and "100"). Lanes 1–3 without DTT, and lanes 4–6 previously reduced with 10 mM DTT. (B) Immunoblotting of 5 μg of immunoprecipitated enzyme per lane with the IF_1 mAb. Where indicated, 20 mM DTT was added to the samples 20 min before loading the gels. (C) Reducing 2D SDS-PAGE of 300 μg of immunoprecipitated F_1F_0I previously cross-linked with 25 μg/mL DSP in SMP. The gel was stained with silver. Two γ spots were vertically aligned with ε and γ (dashed circles). Other cross-linked subunits also appeared corresponding to the second stalk proteins. Those products were not further analyzed. The left standard is purified F_1I complex. The δ subunit was not stained very well in the standard with silver, but it was strongly stained with Coomassie (not shown). (D) The entire lane of nonreducing first dimension containing 20 μg of cross-linked F_1F_0I was excised and subjected to reducing 2D SDS-PAGE to detect the IF_1 products of low-molecular weight. Western blotting with the mAb against IF_1 showed that IF_1 aligned vertically under residual α–IF_1, γ–IF_1, IF–IF_1, and ε–IF_1 cross-linking products. An apparent IF_1 product appeared in the diagonal between ε–IF_1 and $(IF_1)_2$ that was an artifact formed by gel fracture before the transfer. Note the residual IF_1 aggregate of approximately 66 kDa that appears in the left standard lane loaded with pure recombinant IF_1. This band comigrates with the α–IF_1 product of 66 kDa.

(36 kDa) products in the immunoprecipitated F_1F_0I complex. In the 2D gel stained with silver (Fig. 6(A)), the α–IF_1 product was not evident because it was not included in the lane fragment of the 1D gel, or because it was present as a low-yield product. However, other products containing second stalk subunits were also observed in the region of 15–30 kDa after silver staining (Fig. 6(C)). Since some of them have been observed before (Joshi and Burrows, 1990), these were not further analyzed. Taken together, these experiments confirm that the γ–IF_1, ε–IF_1, and

α–IF_1 cross-linked products are not exclusive of the soluble F_1I complex, and they are also formed in the native F_1F_0I complex of the inner mitochondrial membrane.

DISCUSSION

This work shows the closest distance found so far ($\leq$12 Å) between IF_1 and subunits γ and ε of the mitochondrial ATP synthase rotor. Because the γ–IF_1 and ε–IF_1 cross-linkages were obtained with the endogenous IF_1 in the soluble F_1I and in the native F_1F_0I complex, the biological relevance of these results is reinforced. Most of the previous studies have been made with isolated or reconstitued IF_1 in the soluble F_1I complex.

The most important implication of these results is that according to previous proposals (Cabezón *et al.*, 2001; García *et al.*, in press; Lai-Zhang *et al.*, 1999) IF_1 could interfere with the angular movement of the central stalk. For a long time, and on the basis of cross-linking studies (Beltrán *et al.*, 1988; Jackson and Harris, 1988; Klein *et al.*, 1980; Mimura *et al.*, 1993), it has been assumed that IF_1 exerts its inhibitory action by blocking conformational changes of the β subunits. Therefore, our results showing that IF_1 cross-links with stator (α) and rotor (γ, ε) subunits strongly suggest that the primary mechanism of IF_1 may also involve the interference with rotation. These results also suggest that IF_1 may interact with the α/β interfaces, thus IF_1 could interfere with the closure of catalytic α/β interfaces, i.e., resembling the inhibition by aurovertin (Van Raaij *et al.*, 1996). Conversely, the cross-linking of IF_1 with α and β subunits suggests that these interactions could stabilize its association with the stator to resist the drag exerted by the rotor to inhibit ATP hydrolysis. Furthermore, formation of the IF_1–IF_1 cross-linking with endogenous IF_1 in soluble F_1 and whole F_1F_0I complex (Figs. 3 and 6) confirms that IF_1 may exist in a dimerized form in the native enzyme, as suggested by studies with isolated and reconstituted recombinant IF_1 (Cabezón *et al.*, 2000a,b).

Previous studies of phosphorescence decay (Solaini *et al.*, 1997) and of fluorescence resonance energy transfer (FRET) (Baracca *et al.*, 2002) indicated that IF_1 is proximal to ε and γ subunits. FRET studies showed that the N-terminal inhibitory region of IF_1 is closer than its C terminus to the so-called β_E-DELSEED region (Abrahams *et al.*, 1994; Baracca *et al.*, 2002). However, the closest distance found in solube F_1I between γ and reconstituted IF_1 fragments was 50–60 Å (Baracca *et al.*, 2002), a distance 4–5 times larger than the upper limit of 12 Å indicated by our cross-linking data. The 12 Å cross-linking distance of DSP is calculated from its extended structure, therefore it could be shorter if DSP rotates and bends its bonds to cross-link lysines that are closer than 12 Å to each other. Therefore, the γ–IF_1 and γ–ε cross-linkages that we found (Figs. 1–3 and 6) provide the most conclusive structural evidence described so far showing that IF_1 is located at a distance short enough to interfere with rotation of the central stalk. Because γ and ε subunits interact closely to each other in the central stalk (Gibbons *et al.*, 2000), the detection of γ–IF_1 and ε–IF_1 cross-linkages complement each other to confirm the close proximity of IF_1 to the central rotor at a distance $\leq$12 Å. Although the lysine residues involved in these cross-linkages were not determined, a possible docking site of the inhibitory N-terminal region of IF_1 in the F_1-ATPase can be inferred from the current structural data available. As mentioned, according to cross-linking (Jackson and Harris, 1988) and FRET (Baracca *et al.*, 2002) experiments the functionally inhibitory N-terminal portion of IF_1 (Harris, 1997; Lebowitz and Pedersen, 1996; Papa *et al.*, 1996; Van Heeke *et al.*, 1993; Van-Raaij *et al.*, 1990) is closer to the β_E-DELSEED region than to the other β subunits. According to FRET analyses, K24 of this inhibitory domain of IF_1 is closer than the other lysines to the γ subunit (Baracca *et al.*, 2002). Furthermore, K24 is the only lysine of IF_1 that becomes less accessible to chemical modification upon binding to F_1 (Jackson and Harris, 1986). Thus, K24 is the best candidate to be in cross-linking distance to γ, ε, and probably the β_E-DELSEED region. However, the lysine residues of IF_1 actually cross-linked with γ and ε will be determined by the angular position of the rotor relative to IF_1. This relative angular position may also determine the low cross-linking yield observed (Figs. 1–3 and 6) since only those γ and ε subunits properly oriented would cross-link with IF_1. In this line, we used Rasmol 2.6 to accommodate the IF_1 fragment 19–47 derived from the crystal structure of IF_1 H49K (Cabezón *et al.*, 2001) into the β_E/α_E interface of the crystal structure of F_1 interface of the crystal structure of F_1-DCCD (Gibbons *et al.*, 2000) (not shown). We used the orientation of IF_1 suggested by Baracca *et al.* (2002), and we added the restriction of about 12 Å cross-linking distance between IF_1 and γ or ε subunits. The IF_1 19–47 fragment fitted very well in a cleft formed between β_E-DELSEED and the central stalk, with K24 in cross-linking distance to γ and ε subunits. In this or another similar position, IF_1 would interfere with rotation of the central stalk and it also will interact with the α_E/β_E interface. The position of IF_1 in this or another α/β interface is in concordance with previous reports (Cabezón *et al.*, 2001; Stout *et al.*, 1993) suggesting that the inhibitory domain of IF_1 could substitute an homologous β-DELSEED domain by interacting with γ at this "catch" position (Abrahams *et al.*, 1994),

therefore interfering with rotation and possibly with the α/β inter-subunit communication. This or a similar position of IF_1 will also allow changes in α-helical content of the N-terminal and C-terminal regions of IF_1 that are important for the inhibitory action of IF_1 (Lebowitz and Pedersen, 1993, 1996), including formation of a C-terminal antiparallel coiled-coil with another IF_1 (Cabezón *et al.*, 2000a,b) to form F_1I dimers (Cabezón *et al.*, 2000a,b; Domínguez-Ramírez *et al.*, 2001). The mechanism of inhibition of IF_1 could be therefore similar to that of ε subunit of the *E. coli* F_1F_0 complex. The latter subunit works as a ratchet that inhibits rotation only in the ATPase direction by extending its two C-terminal α-helices toward the DELSEED region of a β subunit (Hara *et al.*, 2001; Tsunoda *et al.*, 2001). Because bovine IF_1 cross-links with the β-DELSEED region (Jackson and Harris, 1988) and with γ and ε subunits (Figs. 1 and 2) the overall data suggest that IF_1 could also control rotation of the central stalk by a mechanism similar to that of ε in the *E. coli* ATP synthase. Furthermore, the proton motive force is an important factor since it prevents the productive association of IF_1 with the ATP synthase, therefore favoring the ATP synthase activity of the enzyme (Gómez-Puyou *et al.*, 1979; Harris *et al.*, 1979; Schwersmann and Pedersen, 1981; Van De Stadt *et al.*, 1973).

In summary, this work shows the closest proximity reported between the endogenous IF_1 and the rotor of the soluble F_1I complex. To date, his work provides the more conclusive structural evidence supporting the proposal (Cabezón *et al.*, 2001; García *et al.*, in press; Lai-Zhang *et al.*, 1999) that the inhibitory mechanism of IF_1 may involve the blockade of the angular movement of the rotor in addition to its possible interference with the conformational changes of an α/β catalytic interface. In the whole F_1F_0I complex, IF_1 may be associated to other subunits of the stator and probably of F_0 to resist the rotational drag, therefore adding more stability to the productive binding of IF_1 (García *et al.*, 2000, in press; Papa *et al.*, 2000). It will be important to determine the effect of IF_1 on the rotational movement of the central stalk, and the possible conformational changes that IF_1 experience in the whole ATP synthase to inhibit ATP hydrolysis and favor ATP synthesis *in situ*.

ACKNOWLEDGMENTS

This work was supported by Grant No. J34744-N from CONACyT, México. The critical review of this work is acknowledged to Professors Marietta Tuena de Gómez-Puyou, and Armando Gómez-Puyou from the National University of México. They also kindly provided the antibody directed against the γ subunit. The rat liver IF_1 cloned in pMal-IF_1 in *E. coli* was a generous gift of Prof Roderick A. Capaldi. (Original source: Dr Peter L. Pedersen, The Johns Hopkins University School of Medicine.) Prof. Capaldi also made important suggestions. We thank the help of Leopoldo Gómez-Caudillo with statistical analyses.

REFERENCES

Abrahams, J. P., Leslie, A. G. W., Lutter, R., and Walker, J. E. (1994). *Nature (London)* **370**, 621–628.
Aggeler, R., Coons, J., Taylor, S. W., Gosh, S. S., García, J. J., Capaldi, R. A., and Marusich, M. (2002). *J. Biol. Chem.* **277**, 33906–33912.
Aggeler, R., Ogilvie, I., and Capaldi, R. A. (1997). *J. Biol. Chem.* **272**, 19621–19624.
Baracca, A., Barogi, S., Paolini, S., Lenaz, G., and Solanini, G. (2002). *Biochem. J.* **362**, 165–171.
Beltrán, C., Gómez-Puyou, A., and Tuena de Gómez-Puyou, M. (1988). *Biochem. Biophys. Res. Comm.* **152**, 867–873.
Boyer, P. D. (2000). *Biochim. Biophys. Acta* **1458**, 252–262.
Cabezón, E., Arechaga, I., Jonathan, P., Butler, G., and Walker, J. E. (2000a). *J. Biol. Chem.* **275**, 28353–28355.
Cabezón, E., Butler, P. J., Runswick, M. J., and Walker, J. E. (2000b). *J. Biol. Chem.* **275**, 25460–25464.
Cabezón, E., Runswick, M. J., Leslie, A. G., and Walker, J. E. (2001). *EMBO J.* **20**, 6990–6996.
Capaldi, R. A., and Aggeler, R. (2002). *Trends Biochem. Sci.* **27**, 154–160.
Domínguez-Ramírez, L., Mendoza-Hernández, G., Cárabez-Trejo, A., Gómez-Puyou, A., and Tuena de Gómez-Puyou, M. (2001). *FEBS Lett.* **507**, 191–194.
Duncan, T. M., Bulygin, V. V., Zhou, Y., Hutcheon, M. L., and Cross, R. L. (1995). *Proc. Natl. Acad. Sci. U.S.A.* **92**, 10964–10968.
Feinstein, D. L., and Moundrianakis, E. N. (1984). *J. Mol. Biol.* **259**, 4230–4236.
Fornells, L. A. M., Guimaraes-Motta, N., Neheme, J. S., Martins, O. B., and Silva, J. L. (1998). *Arch. Biochem. Biophys.* **349**, 304–312.
Galante, Y. M., Wong, S.-Y., and Hatefi, Y. (1981). *Biochemistry* **20**, 2671–2678.
García, J. J., Bravo, C., and Minauro-Sanmiguel, F. (in press). In *Recent Research Developments in Bioenergetics* (García, J. J., and Pandalai, S. G., eds.), Transworld Research Network, Trivandrum, India.
García, J. J., Ogilvie, I., Robinson, B. H., and Capaldi, R. A. (2000). *J. Biol. Chem.* **275**, 11075–11081.
García, J. J., Tuena de Gómez-Puyou, M., and Gómez-Puyou, A. (1995). *J. Bioenerg. Biomembr.* **27**, 127–36.
Gibbons, C., Montgomery, M. G., Leslie, A. G. W., and Walker, J. E. (2000). *Nat. Struct. Biol.* **7**, 1055–1061.
Gómez-Puyou, A., Tuena de Gómez-Puyou, M., and Ernster, L. (1979). *Biochim. Biophys. Acta* **547**, 252–257.
Gordon-Smith, D. J., Carbajo, R. J., Ynag, J.-Ch., Videler, H., Runswick, M. J., Walker, J. E., and Neuhaus, D. (2001). *J. Mol. Biol.* **308**, 325–339.
Hara, K. Y., Kato-Yamada, Y., Kikuchi, Y., Hisabori, T., and Yoshida, M. (2001). *J. Biol. Chem.* **276**, 23969–23973.
Harris, D. A. (1997). *Biochim. Biophys. Acta* **1320**, 8–16.
Harris, D. A., Von Tscharner, V., and Radda, G. K. (1979). *Biochim. Biophys. Acta* **548**, 72–84.
Hashimoto, T., Negawa, Y., and Tagawa, K. (1981). *J. Biochem.* (*Tokyo*) **90**, 1151–1157.
Jackson, P. J., and Harris, D. A. (1986). *Biochem. J.* **235**, 577–583.
Jackson, P. J., and Harris, D. A. (1988). *FEBS Lett.* **229**, 224–228.

Joshi, S., and Burrows, R. (1990). *J. Biol. Chem* **265**, 14518–14525.
Kandpal, R. P., and Boyer, P. D. (1987). *Biochim. Biophys. Acta* **890**, 97–105.
Kato-Yamada, Y., Noji., H., Yasuda, R., Kinosita, K., Jr., and Yoshida, M. (1998). *J. Biol. Chem.* **273**, 19375–19377.
Klein, G., Satre, M., Dianoux, A. C., and Vignais, P. V. (1980). *Biochemistry* **19**, 2919–2925.
Klein, G., Satre, M., Dianoux, A. C., and Vignais, P. V. (1981). *Biochemistry* **20**, 1339–1344.
Klein, G., Satre, M., Zaccai, G., and Vignais. P. V. (1982). *Biochim. Biophys. Acta* **681**, 226–232.
Krull, K. W., and Schuster, S. M. (1981). *Biochemistry* **20**, 1592–1598.
Lai-Zhang, J., Xiao, Y., and Mueller, D. M. (1999). *EMBO J.* **18**, 58–64.
Laemmli, U. K. (1970). *Nature* **227**, 680–685.
Lebowitz, M. S., and Pedersen, P. L. (1993). *Arch. Biochem. Biophys.* **301**, 64–70.
Lebowitz, M. S., and Pedersen, P. L. (1996). *Arch. Biochem. Biophys.* **330**, 342–354.
Lopez-Mediavilla, C., Vigny, H., and Godinot, C. (1993). *Eur. J. Biochem.* **215**, 487–496.
Lowry, O. H., Rosegrough, N. J., Farr, A. L., and Randall, R. J. (1951). *J. Biol. Chem.* **193**, 265–275.
Mimura, H., Hashimoto, T., Yoshida, Y., Ichikawa, N., and Tagawa, K. (1993). *J. Biochem. (Tokyo)* **113**, 350–354.
Noji, H., Yasuda, R., Yoshida, M., and Kinosita, K., Jr. (1997). *Nature (London)* **386**, 299–302.
Noji, H., and Yoshida, M. (2001). *J. Biol. Chem.* **276**, 1665–1668.
Papa, S., Zanotti, F., Cocco, T., Perrucci, C., Candita, C., and Minuto, M. (1996). *Eur. J. Biochem.* **240**, 461–467.
Papa, S., Zanotti, F., and Gaballo, A. (2000). *J. Bioenerg. Biomembr.* **32**, 401–411.
Penefsky, H. S. (1979). *Methods Enzymol.* **56**, 527–530.
Pullman, M. E., and Monroy, G. C. (1963). *J. Biol. Chem.* **238**, 3762–3769.
Sabbert, D., Engelbrecht, S., and Junge, W. (1996). *Nature (London)* **381**, 623–625.
Schwerzmann, K., Hullihen, J., and Pedersen, P. L. (1982). *J. Biol. Chem.* **257**, 9555–9560.
Schwerzmann, K., and Pedersen, P. L. (1981). *Biochemistry* **20**, 6305–6311.
Solaini, G., Baracca, A., Gabellieri, E., and Lenaz, G. (1997). *Biochem. J.* **327**, 443–448.
Stout, J. S., Partridge, B. E., Dibbern D. A., and Schuster, S. M. (1993). *Biochemistry* **32**, 7496–7502.
Tsunoda, S. P., Rodgers, A. J. W., Aggeler, R., Wilce, M. C. J., Yoshida, M., and Capaldi, R. A. (2001). *Proc. Natl. Acad. Sci U.S.A.* **98**, 6560–6564.
Tuena de Gómez-Puyou, M., and Gómez-Puyou, A. (1977). *Arch. Biochem. Biophys.* **182**, 82–86.
Valdés, A. M., and Dreyfus, G. (1987). *Biochem. Intl.* **15**, 459–466.
Van De Stadt, R. J., De Boer, B. L., and Van Dam, K. (1973). *Biochim. Biophys. Acta* **292**, 338–349.
Van Heeke, G., Deforce, L., Schinzer, R. A., Shaw, R., Couton., J. M., Shaw, G., Song., P.-S., and Schuster, S. M. (1993). *Biochemistry* **32**, 10140–10149.
Van Raaij, M. J., Abrahams, J. P., Leslie, A. G. W., and Walker, J. E. (1996). *Proc. Natl. Acad. Sci U.S.A.* **93**, 6913–6917.
Van-Raaij, M., Orriss, G. L., Montgomery, G., Runswick, M. J., Fearnley, I. M., Skehel, J. M., and Walker, J. E. (1990). *Biochemistry* **35**, 16618–16625.
Vázquez-Contreras, E., Vásquez-Laslop, N., and Dreyfus, G. (1995). *J. Bioenerg. Biomembr.* **27**, 109–116.